Quantum Computation by Nitrogen-Vacancy centers

Andreas Dietz and Nicolai Lang

Advanced Physics Laboratory Course - 3rd Institute of Physics - UNIVERSITY OF STUTTGART

Universität Stuttgart
Fakultät Mathematik und Physik
FP

Scope of this project

The Deutsch-Jozsa algorithm is commonly considered a touch-stone of quantum computation, that is, it exhibits characteristic features of quantum algorithms such as entanglement of qubits and quantum parallelism. Therefore a realization of this quantum algorithm qualifies the employed physical system as promising candidate for future developements in the field of quantum information processing.

Within the scope of this project, the simplest instance of the Deutsch-Jozsa algorithm was implemented by means of a qutrit realized by the ground state triplet of a single nitrogen-vacancy (NV) center in diamond. Due to the long coherence times of the electronic states in question, the implementation can be realized at room temperature. To this end, we followed the procedure previously published in [2] to reproduce their results.

Theory

■ Theory A | Nitrogen-Vacancy (NV) centers in diamond

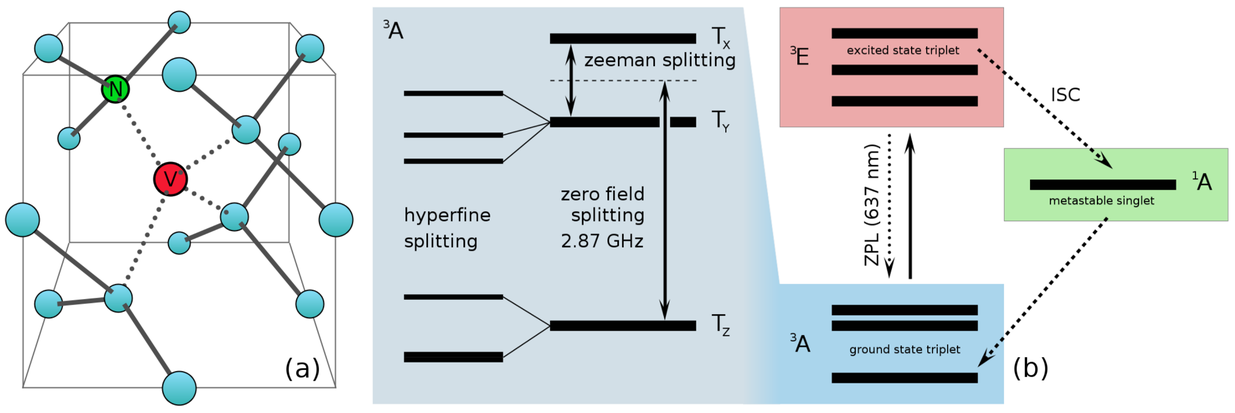

(a) **Crystallographic structure:** Diamond features a fcc-lattice with a two-atomic basis of C-atoms, each beeing surrounded by a tetragonal arrangement of nearest neighbours. A **NV center** is characterized by a missing C-atom (vacancy) and a substitutional adjacent N-atom [see Fig. (a)]. Such defects occur natively but may be implemented artificially as well. NV centers occur charged (uncharged) with six (five) electrons and are denoted by NV^- (NV^0). Here we consider the prevalent NV^- centers.

(b) **Electronic level structure:** Two electrons remain unpaired; their electronic structure is depicted in Fig. (b). The zero field splitting is due to the C_{3v} symmetry of the defect and the hyperfine splitting is caused by the $I = 1$ nuclear spin of the ^{14}N-atom. The lifetimes of the excited states ^{3}E and ^{1}A are 12 ns and several 100 ns, respectively. The latter is populated spin-selectively from $m_S = \pm 1$ by intersystem crossing (ISC) and depopulated spin-selectively to $m_S = 0$. This causes a **spin polarization** in the $m_S = 0$ states (T_z).

■ Theory B | Coherent spin dynamics in NV centers

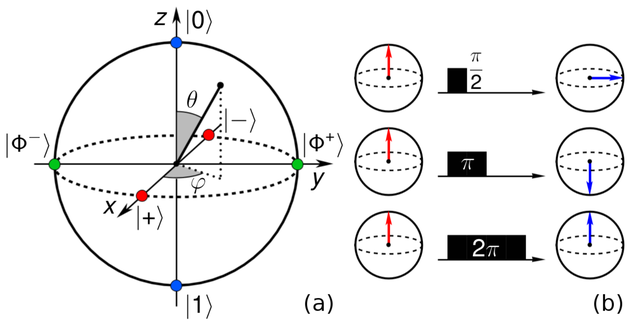

(a) **Two-level systems (qubits):** The state of a qubit can be represented as a point on the Bloch sphere via $|\Psi\rangle = \cos\frac{\theta}{2}|0\rangle + e^{i\varphi}\sin\frac{\theta}{2}|1\rangle$, see Fig. (a).

(b) **Rabi nutations:** A two-level system with energy eigenstates $\{|0\rangle, |1\rangle\}$, energy gap $\hbar\omega_0$, and non-vanishing magnetic dipole moment d may be driven by an RF-field with frequency ω_{mw} and magnetic field B_{mw} rotating in the x-y-plane:

$$\mathcal{H} = -\frac{\hbar\omega_0}{2}\sigma_z - \frac{\hbar\omega_1}{2}\left[\cos(\omega_{\mathrm{mw}}t + \phi)\sigma_x - \sin(\omega_{\mathrm{mw}}t + \phi)\sigma_y\right]$$

(ω_0: Larmor frequency; $\omega_1 \propto dB_{\mathrm{mw}}$: Rabi frequency; ϕ: RF phase)

Transforming in the **rotating frame** via $\exp(-i\omega_{\mathrm{mw}}t\sigma_z/2)$ yields $\mathcal{H}^{\mathrm{rf}} = -\frac{\hbar}{2}(\omega_0 - \omega_{\mathrm{mw}})\sigma_z - \frac{\hbar\omega_1}{2}\left[\cos\phi\,\sigma_x - \sin\phi\,\sigma_y\right]$ which describes for resonant coupling ($\omega_0 = \omega_{\mathrm{mw}}$) **Rabi nutations** on the Bloch sphere with ω_1 around an axis in the x-y-plane with $\varphi = \phi$. E.g. for $\omega_1 t = \pi/2$ and $\Phi = 0$ the transformation $|0\rangle \to |\Phi^+\rangle$ is realized [a so called $\pi/2$-pulse, see Fig. (b)].

■ Theory C | The Refined Deutsch-Jozsa (RDJ) algorithm

- **Problem statement:** Given $f : \{0,1\}^N \to \{0,1\}$; is f **constant**, $2^{-N}\sum_{\mathbf{x}}(-1)^{f(\mathbf{x})} = \pm 1$, or **balanced**, $2^{-N}\sum_{\mathbf{x}}(-1)^{f(\mathbf{x})} = 0$?
- **Classical algorithm:** Worst-case scenario $\hookrightarrow 2^{N-1} + 1$ evaluations of f (exponential growth).
- **Quantum algorithm:** Deutsch-Jozsa algorithm $\hookrightarrow$ requires N qubits and *one* evaluation of f via the unitary operator U_f.
- **Refined Deutsch-Jozsa algorithm:** The original Deutsch-Jozsa algorithm includes a non-entangled qubit due to technical reasons. Removing this qubit requires a redefinition of $U_f \hookrightarrow$ RDJ. One ends up with the following procedure [1]:

1. **Initialization:** $|\Psi_0\rangle = |0\rangle^{\otimes N} \equiv |\mathbf{0}\rangle$
   Start with unentangled N-qubit register.
2. **Hadamard gates (local unitaries):**
   $|\Psi_1\rangle = H^{\otimes N}|\Psi_0\rangle = 1/\sqrt{2^N}\sum_{\mathbf{x}\in\{0,1\}^N}|\mathbf{x}\rangle$
   Superposition representing all possible 2^N bit-strings $\mathbf{x}$.
3. **Application of U_f:** Define unitary U_f: $U_f|\mathbf{x}\rangle := (-1)^{f(\mathbf{x})}|\mathbf{x}\rangle$.
   $|\Psi_2\rangle = U_f|\Psi_1\rangle = 1/\sqrt{2^N}\sum_{\mathbf{x}\in\{0,1\}^N}(-1)^{f(\mathbf{x})}|\mathbf{x}\rangle$
   Amplitudes of $|\Psi_2\rangle$ encode information about f.
4. **Hadamard gates (local unitaries):**
   $|\Psi_3\rangle = H^{\otimes N}|\Psi_2\rangle = 1/2^N\sum_{\mathbf{x},\mathbf{y}\in\{0,1\}^N}(-1)^{f(\mathbf{x})+\mathbf{x}\cdot\mathbf{y}}|\mathbf{y}\rangle$
   Interference renders global information on f accessible.
5. **Measurement:** $P_0 = |\langle\mathbf{0}|\Psi_3\rangle|^2 = 1/2^N\left|\sum_{\mathbf{x}\in\{0,1\}^N}(-1)^{f(\mathbf{x})}\right|^2$
   Obviously $P_0 = 1$ if f = const. and $P_0 = 0$ if f = balanced.
   $\hookrightarrow$ Measuring the register with respect to the computational basis answers the question with certainty.

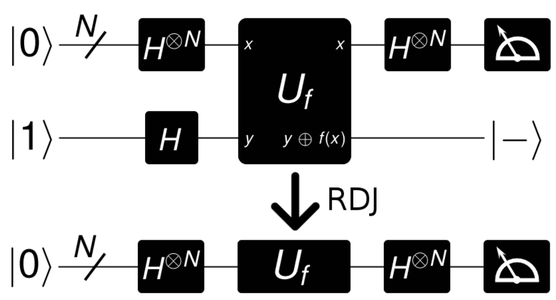

■ Setup | Confocal microscopy of single NVs

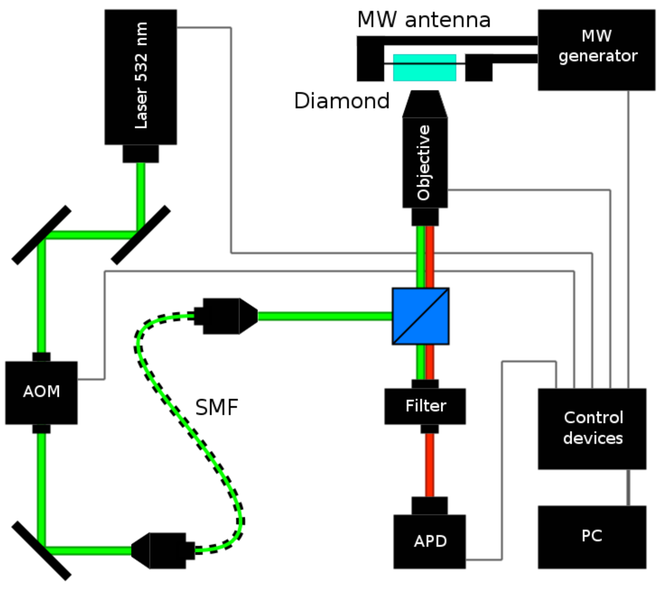

- **Laser:** The diode laser ($\lambda = 532$ nm , $P_{\max} \approx 200$ mW) is used for non-resonant excitation into the phonon band of ^{3}E.
- **AOM:** The acousto-optic modulator is used to generate initialization and read-out pulses.
- **SMF:** To restore a purely gaussian mode, a photonic single-mode fiber is employed (the output of the AOM is not neccessarily a gaussian mode anymore).
- **Objective:** The oil immersion objective is focused from below on the sample holder which is mounted on a 3-axis piezoelectric actuator.
- **MW antenna:** A 20 µm-wire is attached to the diamond and connected to the microwave (MW) generator.
- **Filter:** The filter absorbs the laser reflections from the specimen and transmits the fluorescent light.
- **APD:** The avalance photodiode detects the fluorescence signal.
  (Actually, we use a Hanbury Brown and Twiss setup, i.e., there is a beamsplitter and an additional APD.)

■ References | Further reading

[1] David Collins, K. W. Kim, and W. C. Holton.
Deutsch-jozsa algorithm as a test of quantum computation.
Phys. Rev. A, 58:R1633–R1636, Sep 1998.

[2] Fazhan Shi, Xing Rong, Nanyang Xu, Ya Wang, Jie Wu, Bo Chong, Xinhua Peng, Juliane Kniepert, Rolf-Simon Schoenfeld, Wolfgang Harneit, Mang Feng, and Jiangfeng Du.
Room-temperature implementation of the deutsch-jozsa algorithm with a single electronic spin in diamond.
Phys. Rev. Lett., 105:040504, Jul 2010.

Results

■ Results 1 | Characterizing single NVs

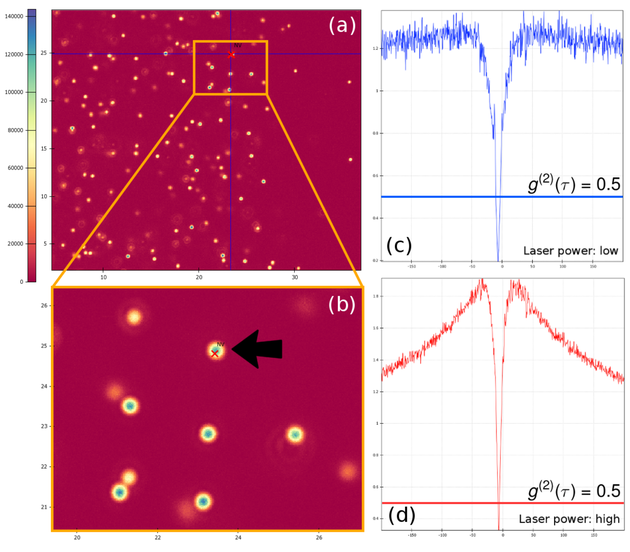

(a) **Overview scan:** This is a 30 µm × 30 µm scan of the sample used for our experiments. It shows the periphery of an NV-rich (left) and an NV-poor (right) region. There are both NV^- and NV^0 centers.

(b) **Detailed scan:** This 7 µm × 7 µm section shows single NVs, some of them with Airy discs (e.g. the left upper one). Centers with different z-position appear out of focus and are therefore darker. The marked NV^- center was used for our measurements.

(c) **Autocorrelation (P_{Laser} low):** NVs are **single-photon emitters**. That is, theoretically the probability of detecting two photons simultaneously vanishes ($\hookrightarrow$ antibunching). The 2nd-order autocorrelation function $g^{(2)}(\tau) = \langle I(t)I(t+\tau)\rangle\langle I(t)\rangle^{-2}$ (I: fluorescence intensity) depicted in Fig. (c) shows the characteristic dip at $\tau = 0$. Since $g^{(2)}(0) < 0.5$ we can be shure that only a **single** NV center contributes to the detected signal.

(d) **Autocorrelation (P_{Laser} hight):** If the laser power is high, intersystem crossing populates the metastable ^{1}A-state ($\hookrightarrow$ shelving). This causes the characteristic bunching shoulders near $\tau = 0$ shown in Fig. (d).

■ Results 2 | Zeeman splitting (CW and pulsed ODMR)

(1) **Zeeman splitting:** By means of a continuous-wave (CW) optically detected magnetic resonance (ODMR), the resonance frequency ($\sim$ 2.87 GHz) was determined. Using this (Larmor) frequency ω_0, the Rabi frequency ω_1 was measured by pulse experiments. With ω_1, pulsed ODMR was possible, shown in Fig. (1a-e). We used a Nd-magnet to adjust the Zeeman splitting and determined $B_z = (h\Delta\nu)/(2g_e\mu_B)$ using the splitting frequency $\Delta\nu$. Due to power broadening, the CW-ODMR spectra cannot resolve the fine structure, see Fig. (1e).

(2) **Fine structure:** In Fig. (2a-c) the Zeeman splitting and the fine structure are shown for low magnetic fields in detail. The field in Fig. (2a) was not artificially applied but is the projection of the earth magnetic field ($B_E = 0.48$ Gs) onto the NV symmetry axis.

(3) **Matrix plot:** Fig. (3a) shows the combined data from Fig. (2a-c) where the fluorescence intensity is colour-coded, the magnetic field varies along the y- and the MW frequency along the x-axis. In Fig. (3b) the same is shown for the data in Fig. (1a-e).

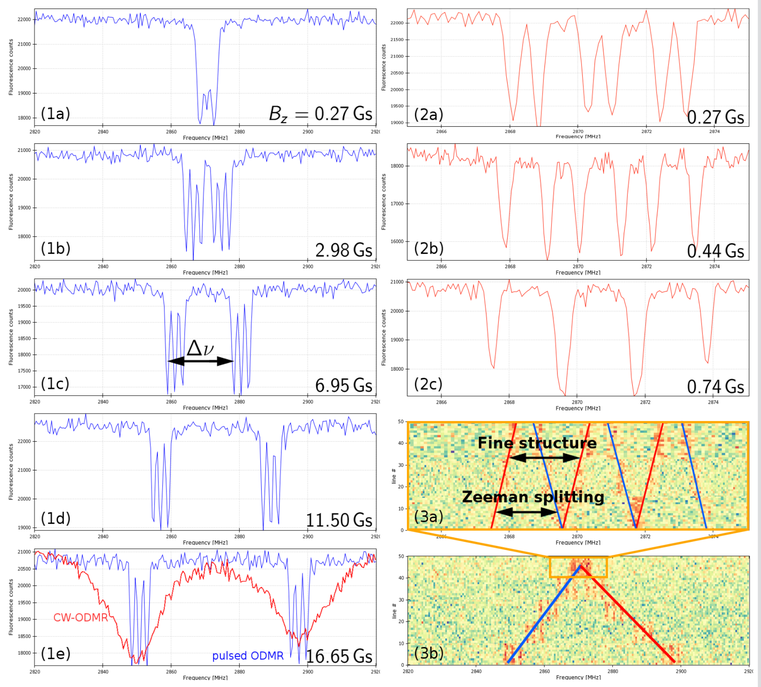

■ Results 3 | Rabi nutations

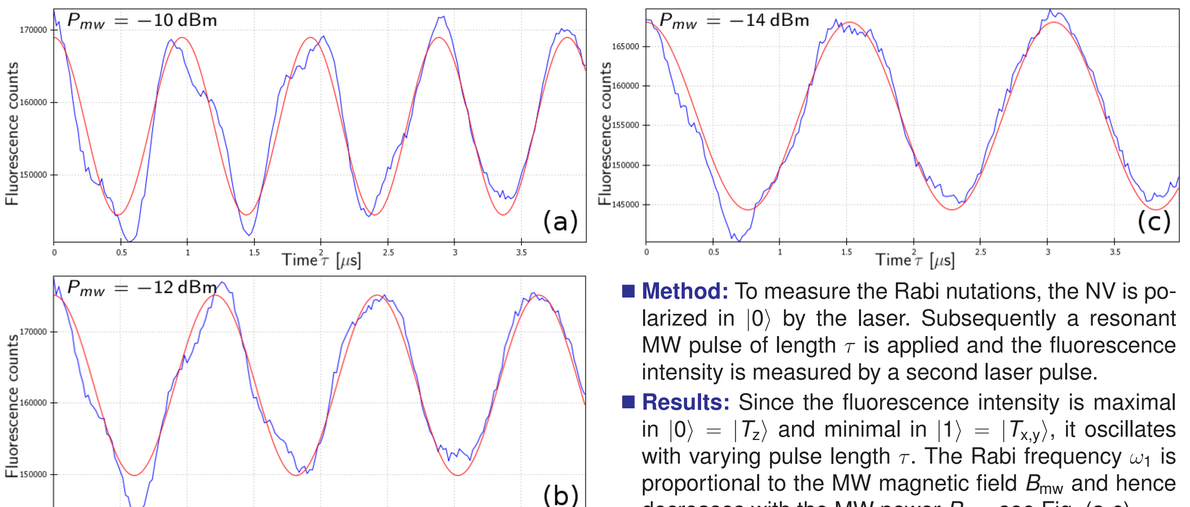

- **Method:** To measure the Rabi nutations, the NV is polarized in $|0\rangle$ by the laser. Subsequently a resonant MW pulse of length τ is applied and the fluorescence intensity is measured by a second laser pulse.
- **Results:** Since the fluorescence intensity is maximal in $|0\rangle = |T_z\rangle$ and minimal in $|1\rangle = |T_{x,y}\rangle$, it oscillates with varying pulse length τ. The Rabi frequency ω_1 is proportional to the MW magnetic field B_{mw} and hence decreases with the MW power P_{mw}, see Fig. (a-c).

■ Results 4 | Implementing the RDJ algorithm

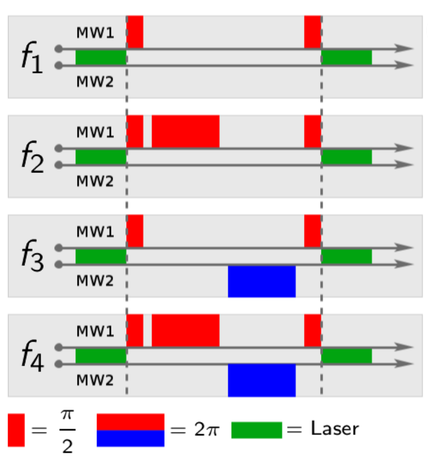

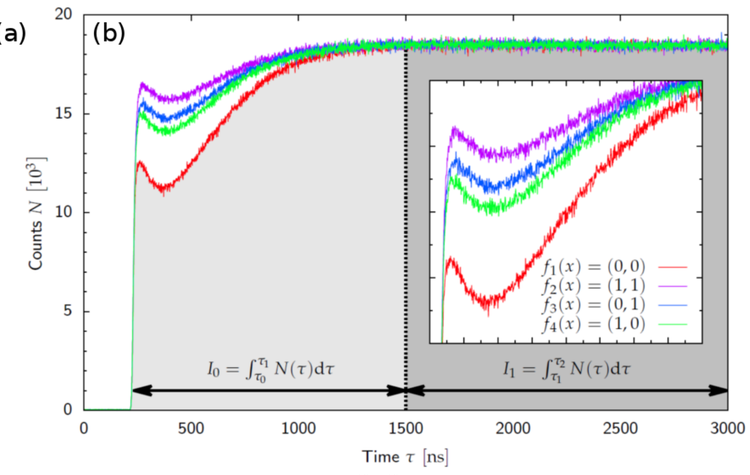

- **Method:** A Zeeman splitting of about $\Delta\nu \approx 600$ MHz was applied. Using two MW generators, the transitions $|T_z\rangle \leftrightarrow |T_x\rangle$ and $|T_z\rangle \leftrightarrow |T_y\rangle$ could be driven separately. The Rabi frequencies of both transitions were measured. Laser pulses at the beginning and at the end of each MW sequence were used to polarize and detect the spin states.
- **Pulse sequences:** We implemented the RDJ for $N = 1$ by means of the four MW pulse sequences depicted in Fig. (a). The $\pi/2$-pulses correspond to the Hadamard gates and the 2π-pulses to U_f.
- **Theoretical expectations:** Let $q_i := I_0^{(i)}/I_1^{(i)}$; then a successful realization of the RDJ implies $q_1 = q_2 < q_3 = q_4$. That is, if f is constant (balanced), the transition $|0\rangle \to |1\rangle$ ($|0\rangle$) is performed which leads to a low (high) fluorescence level right after the MW pulse sequence.
- **Experimental results:** From the integrals $I_0^{(i)}$ and $I_1^{(i)}$ indicated in Fig. (b) we find: $q_1 = 0.72$, $q_2 = 0.79$, $q_3 = 0.78$, and $q_4 = 0.77$; that is, $q_1 < q_3 \approx q_4$ but $q_1 \neq q_2 > q_3 \approx q_4$.
- **Conclusion:**

  We reproduced the implementation of the RDJ algorithm published in [2] except for a single anomaly: Our results for the functions f_1, f_3 and f_4 met the theoretical expectations. However, the fluorescence for f_2 disagreed with theoretical predictions. This may be caused by a faulty measurement of the Rabi frequency or an incorrectly programmed pulse sequence.